Effect of solvents on the extraction and absorption study of natural dye from *Bidens pilosa* for dye-sensitized solar cells

R.R Randela[1], T.S Ranwaha[1] L.M Mathomu[2], R.R Maphanga[3,4] N.E Maluta[1,3]
[1]Physics Department, University of Venda, Thohoyandou, Limpopo 0950, South Africa
[2]Department of Biochemistry and Microbiology, University of Venda, Thohoyandou, 0950, South Africa
[3]National Institute for Theoretical and Computational Sciences (NITheCS), Gauteng 2000, South Africa
[4]Next Generation Enterprises and Institutions Cluster, Council for Scientific and Industrial Research, Pretoria 0001, South Africa

E-mail: ronelronella.randela@univen.ac.za

Abstract. Organic plant-based dye for dye-sensitized solar cells (DSSCs) has gained great interest due to their low cost of manufacturing and environmental friendliness. Most plants in nature contain pigments such as chlorophyll, anthocyanin and betalain that can be used in DSSCs. In this study, the solvents used to extract dye from *B. pilosa* leaves as a sensitizer for DSSC were methanol and water. The dye extracted from *B. pilosa* contained chlorophyll. Methanol was more efficient than water according to the noted absorbance at 665 nm. The molecules responsible for exhibiting a broader range of absorbance is known to be pheophytin found within the chlorophyll extracted from the *B. pilosa* plant. Furthermore, the optical properties using density functional theory (DFT) were computed to optimize the properties of pheophytin. The UV-Vis optimization indicated the absorbance at 450 – 700 nm while the energy gap was observed at 2.06 eV. The experimental and the theoretical UV-Vis analysis outcomes agree, and the study shows that the dye molecule from *B. pilosa* is an efficient sensitizer for DSSCs.

1. Introduction

The utilization of titanium dioxide (TiO_2) as a fundamental semiconductor for the dye-sensitized solar cells has been an included advantage because it can be synthesized utilizing either natural or inorganic strategies. As of now, investigations are towards the green synthesis of TiO_2 to moderate climate change since green synthesis strategies are eco-friendly and non-toxic [1]. The research interest within the field of green nanomaterials has been created exceptionally strong in recent times [2-4]. A strong motivation for this improvement is that nanoparticles regularly have physical and chemical properties different from those made by large-scale materials, which generates a variety of unused potential applications in different areas of innovation [3,4]. Changes in techniques for the era of nanosized powders have been of great significance these days since their properties can include high surface region, high homogeneity, and consistent chemical composition.

DSSCs are mostly sensitized by chemical synthetic dyes since their photoelectric transformation effectiveness can reach 11-12% [5]. However, these kinds of synthetic dyes have high production costs and can effortlessly cause natural contamination; in comparison, natural products and vegetables are

irreplaceable. Besides, they are natural, easily reachable, and cheap. Hence, natural products can decrease the cost of DSSCs and accomplish more economical and natural protection effects.
In this study, the synthesis and characterization of the TiO_2 nanoparticle from *B. pilosa* plant extract was performed. The presence of chlorophyll pigment in the extract was identified with the help of UV-VIS spectroscopy and Fourier Transform Infrared Spectroscopy (FTIR). The characterization studies of TiO_2 nanoparticles were also carried out.

2. Methodology

The study was aimed at comparing the absorption spectra of the 3D pheophytin with pheophytin found within the *B. pilosa* plant (pheophytin) utilizing computational simulations and experimental data.

2.1. Experimental method

2.1.1 Preparation of B. Pilosa plant extracts

The plant was collected at the University of Venda at the site of an agricultural field. The plant was washed using distilled water several times and was left to dry in the laboratory at room temperature until all the moisture contents of the roots were removed. The dried leaves were grinded into fine powder using pestle, mortar, household blender and a small sieve. The extraction process was performed by mixing 10% (w/v) of powder of leaves with methanol in a 50 mL conical tube, similarly, it was done for distilled water. After 24 hours on a rotating platform, the centrifugation process was performed to separate the liquids from the solid-liquid mixture at a speed of 5000 rpm for 15 minutes, finally, the solid residues were filtered using a 0.22µm syringe filter to acquire a purely natural dye solution. The extracts were characterized using a UV-Vis spectrophotometer.

2.1.2 Preparation of TiO_2 nanoparticles

The TiO_2 NPs were prepared by dissolving 5 g of titanium (iv) oxide into 225 ml of distilled water under magnetic stirring for 4 hours. Then, 25 ml of the extracts were slowly added and placed in a shaking incubator machine for 24 hours at room temperature. The colour of the resulting solutions changed from milky white to green after adding the extracts, changed from green to brown after 24 hours. The color change is mainly due to the reduction of the metal ions (Ti^{4+}), which indicates the formation of TiO_2 NPs [6]. The watch glasses were used to dry the solutions in an Ecotherm oven at a temperature of 180 ^oC. The synthesized nanoparticles were characterized using a spectrophotometer, and the dried samples were characterized using a scanning electron microscope (SEM), Fourier Transform Infrared Spectroscopy (FTIR) and X-ray diffraction (XRD)

2.2. Computational method

The structure of the dye molecule was built using Material Studio on a 3D atomistic window. Material Studio software was used for the simulation of the absorption bands and optical absorption, respectively. The optical properties of the dye molecule were performed using first-principles calculations based on density functional theory (DFT), which uses a plane-wave pseudopotential method. We used generalized gradient approximation (GGA) in the scheme of Perdew-Burke-Ernzerhof (PBE) to describe the exchange-correlation function using the coarse quality and all band/EDFT as an electronic minimizer. The calculations of electronic properties of dye molecules were done using Vulnerability Analysis Methodology Program (VAMP)

3. Results and Discussion

3.1. Absorption Spectrum of dye molecules

The absorption spectra of extracted dye from *B. pilosa* using different solvents were compared as shown in Figure 1(A and B) and Figure 2. Chlorophyll extracted from *B. pilosa* indicates the wide absorption which ranges from 350 nm to 700 nm. The absorbance of the dye shows a broad range of wavelength frequency between 395 nm to 665 nm, which is located within visible range, and with three main peaks located at 420, 530 and 665 nm.

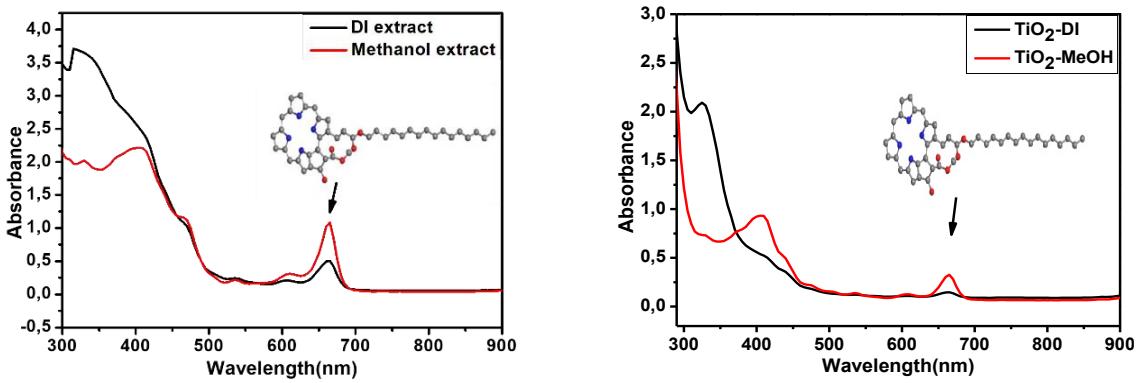

Figure 1(A): The UV-VIS absorption spectra *B.pilosa* extracts. **Figure 1(B)**: The UV-VIS absorptiospectra *B.pilosa* of TiO_2 nanoparticles

Figure 1 (A and B) illustrates the UV-VIS absorption spectra of *B. pilosa* extracted with distilled water and methanol in the visible light spectrum (400-665 nm), respectively. The absorption peak of methanol can be seen at a wavelength of 665 nm, and for distilled water, it is located at 675 nm. The absorption peaks of the dye in this study are like the absorption spectrum of chlorophyll reported previously by [6]. The absorption peak for methanol and distilled water indicates the presence of chlorophyll pigment. B. pilosa is identified to be rich in chlorophyll, and chlorophyll is efficient in photosynthesis [7]. The high absorption peak ranges from 600- 700 nm and a maximum peak absorbance at 665 nm shown it has been known that chlorophyll extracted with distilled water has the broader region of the visible light spectrum in the range of 400 to 675 nm [7] compared to chlorophyll extracted with methanol and is in good agreement with the work reported previous [7,8] since the broader absorption peak of distilled water is at 675 nm. However, in the presence of titanium oxide, the absorbance values of chlorophyll decrease without change in the peak position, as shown in Figure 2. The decrease in the absorption value of chlorophyll upon the addition of titanium dioxide nanoparticles indicates the electronic level interaction of the nanoparticles with the surface of the dye molecules [9,10]. The decrease in the absorbance value also raises the possibility of the adsorption of chlorophyll on the surface of nanoparticles and the formation of a ground state complex of the chlorophyll-titanium oxide. It was also observed that TiO_2 showed absorption only in the UV region with the absorption edge at around 420 nm. The absorption bands of sensitized TiO_2 revealed a redshift; this was mainly caused by the existence of chlorophyll [8].

3.2. The FTIR analysis of synthesized TiO_2 nanoparticles using *B. pilosa*.

FTIR analysis was performed to examine and identify the possible functional groups found in green extraction and green synthesized TiO_2 nanoparticles using the *B. pilosa* plant.

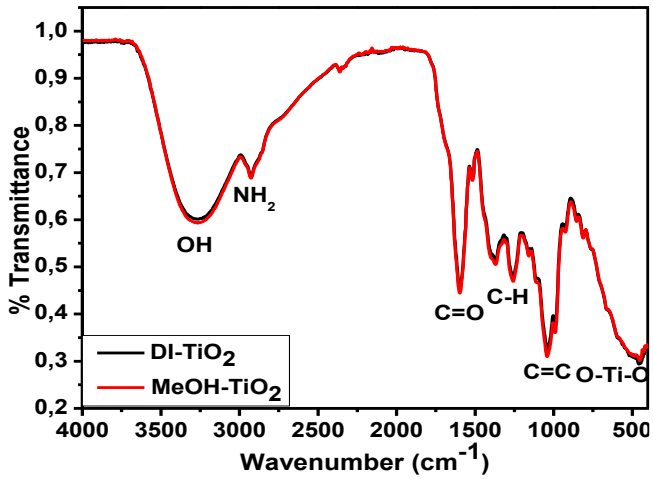

Figure 2. The FTIR analysis of synthesized TiO_2 nanoparticles using *B. pilosa*.

The recorded FTIR spectra of the natural dye extracted from *B. pilosa* indicates most of the characteristic peaks of chlorophyll derivatives such as pheophytin, porphyrin, and chlorins. Chlorophylls and their derivatives have characteristic infrared bands corresponding to C=O, C=C, C-H, and N-H groups. The characteristic C=O band corresponding to the ketone in the cyclopentanone ring of pheophytin is observed at 1735 cm^{-1} for both extracts and extracts synthesized with TiO_2-NPs. Similarly, the C=C vibrations of pheophytin are observed around 1610 cm^{-1} and 1600 cm^{-1} for extracts and synthesis, respectively, which is in good agreement with previous work [10]. Vibrational bands positioned at 2850 cm^{-1} to 2927 cm^{-1} have contributed to the N-H stretching of amide II [10]. The region of 1310 cm^{-1} and 1376 cm^{-1} are contributed to the amide III vibration and the H-C-H [10,11] the wavenumber at 1225 cm^{-1} is assigned to the stretching vibrations of the C-O for the ester groups [6,11] FTIR spectral analysis also confirms the presence of pheophytin in *B. pilosa* extracts, which is well-matched with the UV–VIS obtained in figure 1.

3.3. SEM, TEM and EDS Analysis

The morphological features of the prepared nanoparticles were performed using TEM and SEM. Figure 4 (A and B) indicates the TEM and SEM images of synthesized nanoparticles using *B. pilosa* leaf extracts

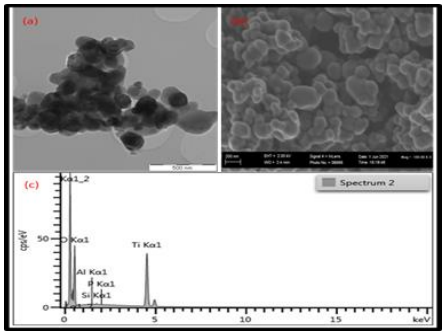

Figure 4(A): Water: (a) TEM, (b)SEM, (c) EDS

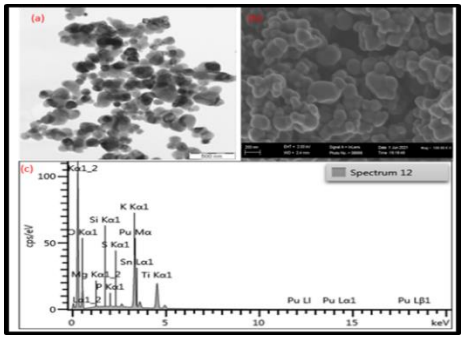

Figure 4(B): Methanol: (a) TEM, (b)SEM, (c) EDS

The TEM and SEM images of synthesized nanoparticles indicate the particles being distributed in a spherical shape, even though some aggregation and agglomeration were observed. The tendency of the particles to agglomerate was directly related to the crystal size obtained, EDS analysis indicates the presence of the elements such as Ti and O, which confirms the presence of TiO_2 NPs and other elements were found on EDS elements such as potassium (K), aluminum (Al) and silicon (Si) were observed for both water and methanol; magnesium (Mg), Plutonium (Pu), Si, K and Al were observed. These are elements that can possibly be found in a *B. Pilosa* plant. The results of this study are consistent with other studies that have reported detection of elemental Ti at 5 keV [12,13].

3.4. XRD analysis of synthesized TiO_2 NPs

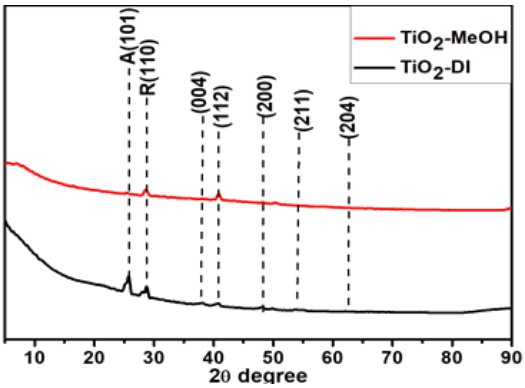

Figure 5. XRD analysis of synthesized TiO_2 NPs using *B. pilosa.*

XRD patterns of TiO_2 nanocrystalline are shown in Figure 5. A relatively short 2θ range (22 – 30°) and small scan rate were chosen. For each pattern, there was a peak at about 25.4◦, which is marked as anatase (1 0 1). No peaks could be found with respect to the other two phases of TiO_2, that is rutile and brookite. The result corresponds to that obtained in SEM studies in Figure 4 (A and B), which is in good agreement with previous studies [8]. Several peaks were observed (1 0 1), (0 0 4), (2 0 0), (2 0 4), demonstrating the anatase phase TiO_2 for all the cases [9].

3.5. *Energy level and isodensity of the Porphyrin dye*

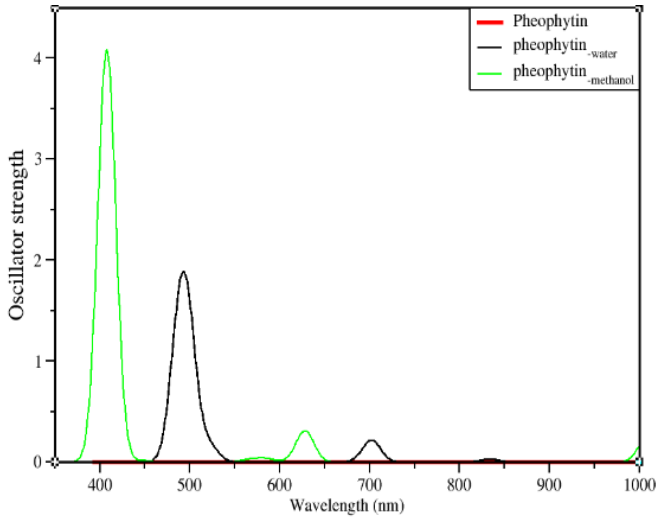

Figure 6. The UV-VIS absorption spectra of a pheophytin molecule

In figure 6, pheophytin shows a lower absorbance of sunlight in both the visible region and near-infrared region with a lower oscillator strength resulting in lower efficiency however, with the addition of the effect of solvents introduced on the pheophytin dye molecule, it is observed that methanol solvent absorbs more sunlight at a higher oscillating strength resulting in obtaining higher efficiency in the visible region. Methanol has a higher absorbance in the visible region at 405 and 407 nm, and water at 494 nm. This is in good agreement with the previous work [14]. Computational and experimental absorbance are comparable with each other since the pheophytin molecule has an absorbance in both visible and near-infrared regions and can be observed in Figure 1(A) and Figure 6 for both absorbance spectra.

The HOMO-LUMO energy gap of a pheophytin molecule was calculated using the following equation

$$\mathbf{E_{gap} = HOMO - LUMO} \quad (1)$$

Where E_{gap} is the energy gap

Table: 1 HOMO-LUMO energy levels of dye molecules

	HOMO	LUMO	$\mathbf{E_{gap}}$ **(eV)**
Pheophytin	-7.656	-5.596	2.06
Pheophytin-$_{water}$	-8.391	-5.596	2.7
Pheophytin-$_{methanol}$	-8.568	-5.02	3.5

The HOMO and LUMO energies of pheophytin and pheophytin with the effect of solvents are shown in Table 1. The HOMO–LUMO energy gap values for pheophytin are 2.06 eV, while for pheophytin with the effect of solvents (methanol, water) are 3.5 eV and 2.7 eV, respectively, which agrees well

with the HOMO and LUMO values reported [15] on a photoactive layer of DSSCs based on natural dyes. The lower HOMO-LUMO energy gap of the sensitizer enhances absorption at higher wavelengths and the photocurrent response of DSSCs. The lower energy gap between the HOMO and LUMO of sensitizer enhances the absorption of photons in higher spectral regions of the solar spectrum. The pheophytin dye molecule has a relatively low HOMO-LUMO energy gap of 2.06 eV, which will facilitate electron excitation. A high HOMO energy indicates that high compounds/molecules facilitate electron transfer, so that chemical bonds will be easily formed. High LUMO energy for dye molecules will facilitate the injection of electrons from the semiconductor so that the recombination of dye to the ground level will be faster. In dye molecules with relatively low HOMO-LUMO energy, pheophytin and pheophytin-methanol show the basis for determining the ability of a molecule to become a sensitizer in DSSCs, and are comparable to the literature [14,15].

4. Conclusion

Computational first-principle calculations were based on the density functional theory to investigate the electronic and optical properties of pheophytin dye molecules extracted from the *B. pilosa* plant leaves. The outcomes of the study show that the extracted dye has a lesser Homo-Lumo gap compared to the band gap of semiconductors that are used in the DSSCs application. The UV-VIS absorption spectrum shows absorption peaks in the visible to near-infrared, which gives evidence for photo absorption in those regions. Hence, it is concluded that the use of dye extract from *B. pilosa* can enhance the performance of DSSCs

5. Acknowledgement

This work was supported through the NRF Thuthuka and National Institute for Theoretical Physics (NITHECS). We would like to thank the University of Venda for the support to carry out this research and the Center for High Performance Computing (CHPC) for access to their computing facility.

References

[1] Sharma, S., Uttam, R., & Uttam, K. N. (2020). Interaction of chlorophyll with titanium dioxide and iron oxide nanoparticles: A temperature-dependent fluorescence quenching study. Analytical Letters, 53(12), 1851-1870.

[2] Krishnan, S., & Shriwastav, A. (2021). Application of TiO_2 nanoparticles sensitized with natural chlorophyll pigments as catalyst for visible light photocatalytic degradation of methylene blue. Journal of Environmental Chemical Engineering, 9(1), 104699.

[3] Gour, A., & Jain, N. K. (2019). Advances in green synthesis of nanoparticles. Artificial cells, nanomedicine, and biotechnology, 47(1), 844-851.

[4] Zoccal, J. V. M., Arouca, F. O., & Gonçalves, J. A. S. (2010). Synthesis and characterization of TiO_2 nanoparticles by the method pechini. In Materials science forum (Vol. 660, pp. 385-390). Trans Tech Publications Ltd.

[5] Chiba, Y., Islam, A., Watanabe, Y., Komiya, R., Koide, N., & Han, L. (2006). Dye-sensitized solar cells with conversion efficiency of 11.1%. Japanese journal of applied physics, 45(7L), L638

[6] Ahmad, W., Jaiswal, K. K., & Soni, S. (2020). Green synthesis of titanium dioxide (TiO_2) nanoparticles by using Mentha arvensis leaves extract and its antimicrobial properties. Inorganic and Nano-Metal Chemistry, 50(10), 1032-1038.

[7] Mahmoud, S., Mohamed, B. S., & Killa, H. (2021). Synthesis of different sizes TiO_2 and photovoltaic performance in dye sensitized solar cell. Frontiers in Materials, 385.

[8] Torchani, A., Saadaoui, S., Gharbi, R., & Fathallah, M. (2015). Sensitized solar cells based on natural dyes. Current Applied Physics, 15(3), 307-312.

[9] Syafinar, R., Gomesh, N., Irwanto, M., Fareq, M., & Irwan, Y. M. (2015). Chlorophyll pigments as nature-based dye for dye-sensitized solar cell (DSSC). Energy Procedia, 79, 896-902.*Ene*

[10] Ramanarayanan, R., Nijisha, P., Niveditha, C. V., & Sindhu, S. (2017). Natural dyes from red amaranth leaves as light-harvesting pigments for dye-sensitized solar cells. Materials research bulletin, 90, 156-161.

[11] Shanmugam, V., Manoharan, S., Sharafali, A., Anandan, S., & Murugan, R. (2015). Green grasses as light harvesters in dye sensitized solar cells. Spectrochimica Acta Part A: Molecular and Biomolecular Spectroscopy, 135, 947-952..

[12] Li, Y., Li, H., Song, P., & Sun, C. (2015). Photoactive layer of DSSCS based on natural dyes: a study of experiment and theory. Journal of Nanomaterials, 2015.

[13] Pawar, M., Topcu Sendoğdular, S., & Gouma, P. (2018). A brief overview of TiO_2 photocatalyst for organic dye remediation: case study of reaction mechanisms involved in Ce-TiO_2 photocatalysts system. Journal of Nanomaterials, 2018.
[14] Rahmatika, Z. (2021, February). Theoretical Modification of Pheophytin Using Cu, Ni, and Zn Atoms as a Sensitizer for Dye Sentized Solar Cell (DSSC). In Journal of Physics: Conference Series (Vol. 1788, No. 1, p. 012006). IOP Publishing.
[15] Hasegawa, J., Ozeki, Y., Ohkawa, K., Hada, M., & Nakatsuji, H. (1998). Theoretical study of the excited states of chlorin, bacteriochlorin, pheophytin a, and chlorophyll a by the SAC/SAC− CI method. The Journal of Physical Chemistry B, 102(7), 1320-1326.